

Ceric phosphates and nanocrystalline ceria: selective toxicity to melanoma cells

Taisiya O. Kozlova^{1,a}, Anton L. Popov^{2,b}, Mikhail V. Romanov^{2,c}, Irina V. Savintseva^{2,d},
Darya N. Vasilyeva^{1,3,e}, Alexander E. Baranchikov^{1,f}, Vladimir K. Ivanov^{1,g}

¹Kurnakov Institute of General and Inorganic Chemistry of the Russian Academy of Sciences, Moscow, Russia

²Institute of Theoretical and Experimental Biophysics of the Russian Academy of Sciences, Pushchino, Russia

³National Research University Higher School of Economics, Moscow, Russia

^ataisia.shekunova@yandex.ru, ^bantonpopovleonid@gmail.com, ^crmvya@yandex.ru, ^dsavintseva_irina@mail.ru,

^ednavasileva.1@edu.hse.ru, ^fa.baranchikov@yandex.ru, ^gvan@igic.ras.ru

Corresponding author: Taisiya O. Kozlova, taisia.shekunova@yandex.ru

PACS 61.66.Fn; 81.70.-q; 87.17.-d

ABSTRACT Nanocrystalline cerium dioxide is a promising inorganic UV filter for sunscreen applications due to its high UV absorbance and non-toxicity to normal cells. Nanoscale CeO₂ also showed selective cytotoxicity to cancer cells, thus ceria-containing materials are now regarded for the creation of both preventive and therapeutic compositions. At the same time, the interaction of ceria nanoparticles with cell membranes and phosphate-rich components of sunscreen compositions arise the interest to biocompatibility of ceric phosphates. Crystalline cerium(IV) phosphates can be a promising alternative for nanoscale CeO₂ due to their low solubility, high redox stability and UV protective property. However, to date, there is no information on their toxicity to cancer cells. In this work, using the MTT, Live/Dead and MMP assays, we demonstrated for the first time that the inhibitory impact of ceric phosphates Ce(PO₄)(HPO₄)_{0.5}(H₂O)_{0.5} and NH₄Ce₂(PO₄)₃ on murine melanoma B16/F10 cell line *in vitro* is comparable to that of nanoscale CeO₂, at high (500–1000 μg/ml) concentrations.

KEYWORDS ceric phosphates, ceria, metabolic activity, reactive oxygen species, UV protectors.

ACKNOWLEDGEMENTS This work was supported by Russian Science Foundation (Grant no. 21-73-00294, <https://rscf.ru/en/project/21-73-00294/>) using the equipment of the JRC PMR IGIC RAS.

FOR CITATION Kozlova T.O., Popov A.L., Romanov M.V., Savintseva I.V., Vasilyeva D.N., Baranchikov A.E., Ivanov V.K. Ceric phosphates and nanocrystalline ceria: selective toxicity to melanoma cells. *Nanosystems: Phys. Chem. Math.*, 2023, **14** (2), 223–230.

1. Introduction

Cerium is one of the most common elements among rare earth metals, and, unlike most representatives of this group, is stable in two oxidation states, +3 and +4 [1,2]. Among the inorganic cerium compounds, ceria (CeO₂) is regarded as the most promising for practical uses [3]. In particular, cerium dioxide is a part of automotive three-way catalysts, it is used as the main component of polishing mixtures and abrasives, solid oxide fuel cells and protective anticorrosion coatings, it possesses high activity in a wide range of catalytic applications [4–7].

In the nanodispersed state, CeO₂ exhibits unique redox activity, acts as an inorganic antioxidant capable of protecting living systems from oxidative stress, and can perform the functions of certain enzymes – oxidoreductases, phosphatases, etc. [8–10].

In addition to outstanding biological activity, nanodispersed CeO₂ shows high light absorption in the UV range, which allows one to consider it as a promising component of sunscreen cosmetics instead of photocatalytically active nanocrystalline TiO₂ and ZnO [11–14]. Excessive exposure to sunlight, especially ultraviolet light, has been found to be harmful to the skin and can lead to photosensitivity, erythema and burns, premature aging, and even cancer [15]. A number of studies have shown that nanosized cerium dioxide exhibits selective cytotoxicity with respect to cancer cells [16–18], including skin cancer cells (e.g. melanoma) [19–21], which makes it attractive not only as a prophylactic agent, but also as a therapeutic. However, the use of nanodispersed CeO₂ in sunscreens has certain disadvantages. At a natural skin pH (~5), CeO₂ can act as prooxidant [22,23], negatively affecting the skin health. Moreover, even if the beneficial antioxidant properties of nanodispersed cerium dioxide are retained on skin surface, they can be lost due to the interaction of CeO₂ with phosphate groups presented in sunscreen components or in cell membranes [24–26]. Cerium dioxide is extremely prone to catalytic oxidation of organic compounds [27–29].

In turn, due to their low solubility and high redox stability, cerium phosphates are not expected to interact with organic compounds presented in sunscreens, thus allowing to obtain highly stable formulations with long shelf life [30,31]. High

biocompatibility of the phosphate matrix, along with high ultraviolet absorption and low photocatalytic activity of cerium phosphates, provide interest in these compounds as promising inorganic UV filters [32–38].

In our previous report [39], a comprehensive study of the sun protection characteristics and cytotoxicity of amorphous and crystalline cerium(IV) phosphates $\text{Ce}(\text{PO}_4)(\text{HPO}_4)_{0.5}(\text{H}_2\text{O})_{0.5}$ and $\text{NH}_4\text{Ce}_2(\text{PO}_4)_3$ was performed for the first time. It was shown that $\text{NH}_4\text{Ce}_2(\text{PO}_4)_3$ is characterised by SPF (2.7) and UVAPF (2.5) values close to the corresponding characteristics of the well-known inorganic UV filters, nanocrystalline CeO_2 and TiO_2 . Moreover, in a wide range of concentrations, crystalline cerium (IV) phosphates were found to be not toxic to NCTC L929 mouse fibroblast cells and human mesenchymal stem cells, and even enhanced the proliferative activity of the latter.

In this work, we studied the effect of the same crystalline cerium(IV) phosphates, $\text{Ce}(\text{PO}_4)(\text{HPO}_4)_{0.5}(\text{H}_2\text{O})_{0.5}$ and $\text{NH}_4\text{Ce}_2(\text{PO}_4)_3$, on skin cancer cells (melanoma) in order to detect their possible selective cytotoxicity with respect to transformed cells. The toxicity evaluation of ceric phosphates to the cells is of primary importance for understanding the cytotoxicity mechanisms of CeO_2 nanoparticles, especially in biological phosphate-rich media.

2. Experimental Section

The following materials were used as received, without further purification: $\text{Ce}(\text{NO}_3)_3 \cdot 6\text{H}_2\text{O}$ (pure grade, Lanhit Russia), phosphoric acid (85 wt.% aq, $\rho = 1.689 \text{ g/cm}^3$, extra-pure grade, Komponent-Reaktiv Russia), aqueous ammonia (25 wt.%, extra-pure grade, Khimmed Russia), isopropanol (extra-pure grade, Khimmed Russia), distilled water.

First, nanocrystalline CeO_2 , which was also further used for the synthesis of cerium(IV) phosphates, was obtained in accordance with previously published procedure [40]. Briefly, 0.08 M cerium(III) nitrate solution in aqueous isopropanol (water : isopropanol = 1 : 1 v/v) was mixed with 3 M aqueous ammonia. The obtained yellow precipitate was washed with distilled water to a neutral pH and dried at 60°C.

To obtain crystalline ceric phosphates, 0.1 g of nanocrystalline cerium dioxide was dissolved in concentrated phosphoric acid (5 ml) at 80°C. For the synthesis of $\text{Ce}(\text{PO}_4)(\text{HPO}_4)_{0.5}(\text{H}_2\text{O})_{0.5}$ or $\text{NH}_4\text{Ce}_2(\text{PO}_4)_3$, to the cooled solution, 35 ml of distilled water or 1.5 M aqueous ammonia was added under vigorous stirring. The resulting gel-like precipitates (~40 ml) were placed in 100 ml Teflon autoclave and subjected to hydrothermal treatment at 180°C for 24 h. After cooling the autoclave, the precipitates were repeatedly washed using distilled water and dried at 60°C in air.

Powder X-ray diffraction (PXRD) patterns were acquired on a Bruker D8 Advance diffractometer, using $\text{Cu K}_{\alpha 1,2}$ radiation in the 2θ range of 5°–80° with 0.02° 2θ step and a signal accumulation time of no less than 0.2 s per point.

Scanning electron microscopy (SEM) images were obtained using a Carl Zeiss NVision 40 high-resolution electron microscope equipped with an Oxford Instruments X-MAX detector (80 mm²) at an accelerating voltage of 1–2 kV.

Transmission electron microscopy (TEM) images were collected using a Leo912 AB Omega microscope. The images were obtained at an accelerating voltage of 100 kV in a bright field mode with magnifications up to $\times 500\,000$.

The cytotoxicity of nanoscale ceria and crystalline cerium(IV) phosphates were assessed *in vitro* using a murine melanoma B16/F10 cell line. The cells were seeded in 96-well plates at a density of 30 000 cells per cm² in a DMEM/F12 nutrient (culture) medium containing 10% fetal bovine serum. After 12 h of cultivation, the culture medium was completely replaced with an identical medium containing the suspension of cerium(IV) phosphates or CeO_2 prepared under intense magnetic stirring for 30 min. The concentration of the solid particles in DMEM/F12 medium was fairly high, 500 or 1000 $\mu\text{g/ml}$ to test their acute toxicity and to be close to the concentrations of inorganic UV filters used in sunscreen formulations. In a control experiment, the culture medium was replaced with a fresh medium that did not contain either cerium(IV) phosphates or ceria. After 24, 48 or 72 h of incubation, the nutrient medium with the test substances was replaced with a serum-free culture medium DMEM/F12 containing 3-[4,5-dimethylthiazol-2-yl]-2,5-diphenyltetrazolium bromide (MTT) at a concentration of 500 $\mu\text{g/ml}$. After 3 h, the medium with MTT was removed and dimethyl sulfoxide (DMSO) was added. The plates were shaken at room temperature for 10 min to dissolve formazan crystals. The optical density of the formazan was measured on a BIO-RAD 680 photometer at 540 nm. The optical density values were recalculated as percentages of the control group. Statistical data processing was performed using GraphPad Prism software. Statistically significant differences were determined in accordance with the Welch's *t*-test at $0.01 < p < 0.05$ (*), $0.001 < p < 0.01$ (**), $0.0001 < p < 0.001$ (***) and $p < 0.0001$ (****). The IC_{50} value (half maximal inhibitory concentration) was used as the boundary for determining the cytotoxicity of the samples.

To assess the proportion of dead cells after incubation with the tested substances, Live/Dead assay was conducted. After 24, 48 or 72 h culture medium containing ceric phosphates or ceria was replaced with Hanks' balanced salt solution containing a mixture of fluorescent dyes Hoechst 33342 (binds to the DNA of all cells, $\lambda_{ex} = 350 \text{ nm}$, $\lambda_{em} = 460 \text{ nm}$) and propidium iodide (binds to the DNA of dead cells, $\lambda_{ex} = 535 \text{ nm}$, $\lambda_{em} = 615 \text{ nm}$). After 15 min, the cells were washed with Hanks' balanced salt solution and then analysed using a BioRad Zee fluorescence microscope. The micrographs were further processed with ImageJ software.

To analyze the level of membrane mitochondrial potential (MMP), mitochondria were stained using a voltage-sensitive dye tetramethylrhodamine (TMRE; Lumiprobe, Russia). After 24, 48 or 72 h, the culture medium containing the tested substances was replaced with TMRE solution at 500 nM concentration ($\lambda_{ex} = 552 \text{ nm}$, $\lambda_{em} = 574 \text{ nm}$), then the cells were twice washed by Hanks' balanced salt solution. The analysis of the cells was performed using a BioRad Zee fluorescence microscope and micrographs were further processed with ImageJ software. The fluorescence intensity values

were recalculated as percentages of the control group. Statistically significant differences were determined in accordance with the Welch's *t*-test at $0.01 < p < 0.05$ (*), $0.001 < p < 0.01$ (**), $0.0001 < p < 0.001$ (***) and $p < 0.0001$ (****) using GraphPad Prism software.

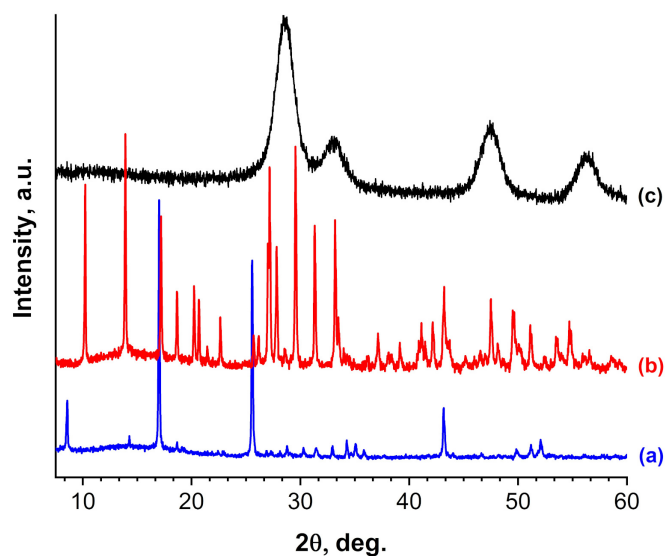


FIG. 1. Diffraction patterns for a) $\text{Ce}(\text{PO}_4)(\text{HPO}_4)_{0.5}(\text{H}_2\text{O})_{0.5}$, b) $\text{NH}_4\text{Ce}_2(\text{PO}_4)_3$, c) CeO_2

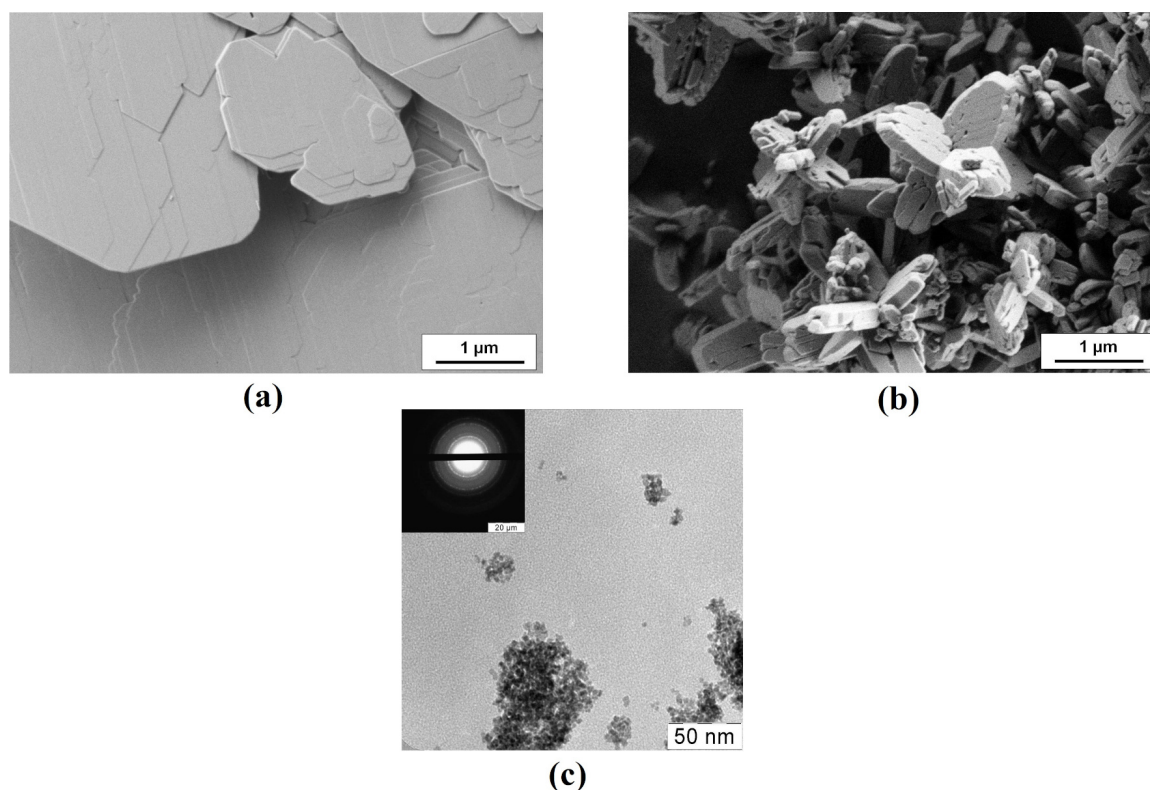


FIG. 2. SEM images for a) $\text{Ce}(\text{PO}_4)(\text{HPO}_4)_{0.5}(\text{H}_2\text{O})_{0.5}$, b) $\text{NH}_4\text{Ce}_2(\text{PO}_4)_3$, and TEM image for c) CeO_2

3. Results and discussion

The diffraction patterns of the obtained crystalline cerium(IV) phosphates show the sets of reflections corresponding to single-phase $\text{Ce}(\text{PO}_4)(\text{HPO}_4)_{0.5}(\text{H}_2\text{O})_{0.5}$ or $\text{NH}_4\text{Ce}_2(\text{PO}_4)_3$ (Fig. 1a,b) [41, 42]. The diffraction pattern of cerium oxide is typical to this compound in a nanocrystalline state and shows phase purity of the material (Fig. 1c). According to SEM data, $\text{Ce}(\text{PO}_4)(\text{HPO}_4)_{0.5}(\text{H}_2\text{O})_{0.5}$ phase consisted of lamellar thin (~ 100 nm) aggregates, while $\text{NH}_4\text{Ce}_2(\text{PO}_4)_3$

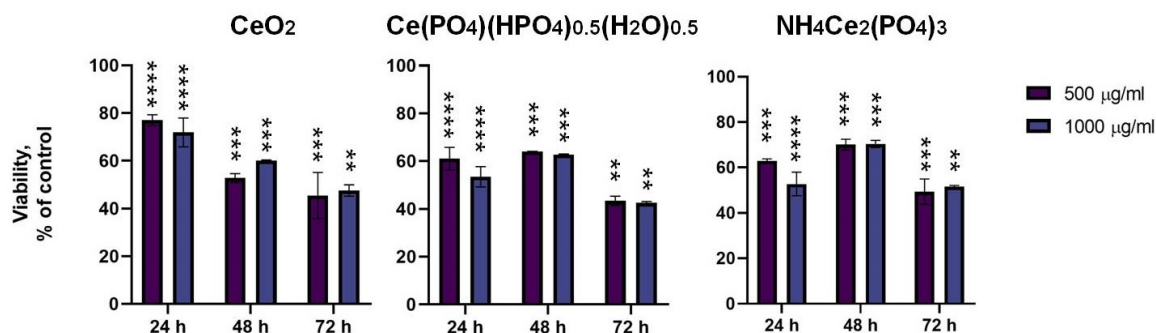


FIG. 3. The metabolic activity of B16/F10 murine melanoma cell line after 24–72 h of cultivation with cerium(IV) phosphates and ceria in concentrations of 500 or 1000 $\mu\text{g/ml}$. The data are presented as mean \pm standard deviation, $0.001 < p < 0.01$ (**), $0.0001 < p < 0.001$ (***) and $p < 0.0001$ (****) via Welch's *t*-test

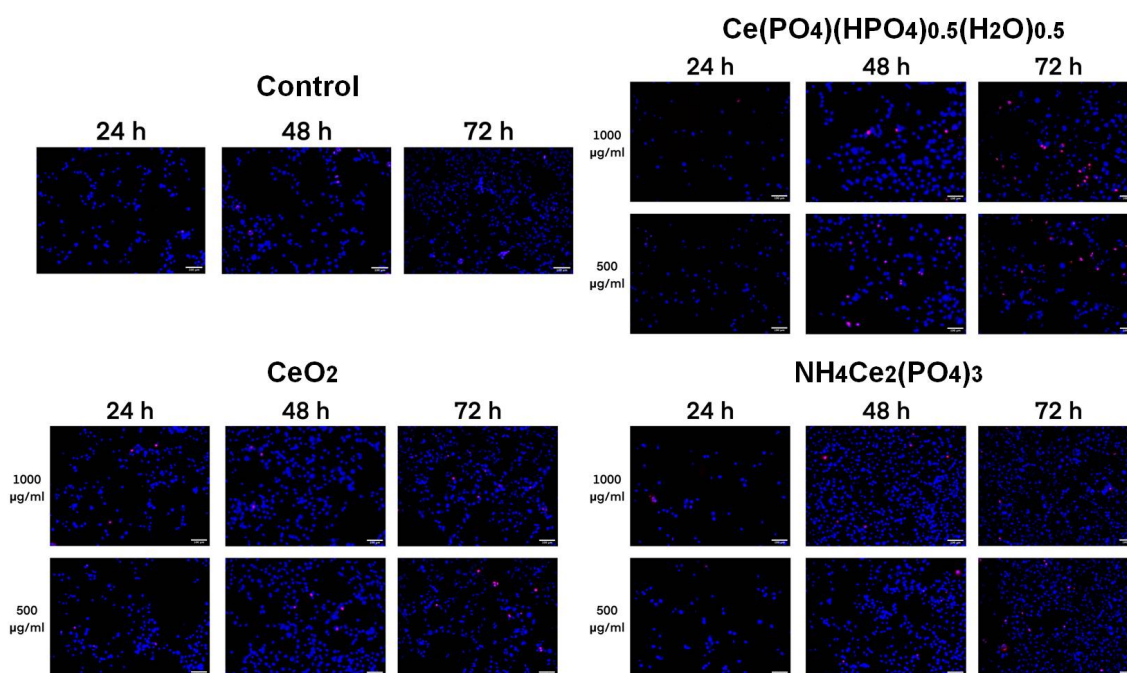


FIG. 4. Live/Dead assay of B16/F10 murine melanoma cells in the presence of ceria or cerium(IV) phosphates. Hoechst 33342 (blue) and propidium iodide (red) staining. Scale bar – 100 μm

phase consisted of elongated microparticles (Fig. 2a,b). The TEM images of CeO₂ show nanoparticles with a size of about 5 nm (Fig. 2c), which is in a good agreement with the estimates made from the results of PXRD data.

The study of the metabolic activity of B16/F10 murine melanoma cells using the MTT assay showed that the activity of NADPH-dependent oxidoreductases after 24 h of co-incubation with ceria nanoparticles decreased to 70–80% in comparison with the control group, while co-incubation of the cells with Ce(PO₄)(HPO₄)_{0.5}(H₂O)_{0.5} and NH₄Ce₂(PO₄)₃ reduced in to 60% (Fig. 3). After 48 h co-incubation of melanoma cells with nanocrystalline cerium dioxide, their viability level reached 60% relatively to the control group, while in the case of cerium(IV) phosphates, there was no additional decrease in metabolic activity compared to the 24 h experiment. After 72 h, the metabolic activity of B16/F10 murine melanoma cells decreased to the IC₅₀ value for all the test samples. Thus, Ce(PO₄)(HPO₄)_{0.5}(H₂O)_{0.5} and NH₄Ce₂(PO₄)₃, along with cerium dioxide, significantly inhibit the viability of B16/F10 cancer cells. At the same time, the inhibitory effect of both of the cerium(IV) phosphates is almost identical, which indirectly indicates that their cytotoxicity is not due to the microstructure and microenvironment of Ce(IV) in crystal lattice.

The results of the Live/Dead assay (Fig. 4) demonstrate that co-incubation of B16/F10 murine melanoma cells with nanocrystalline CeO₂ or cerium(IV) phosphates at concentrations of 500 or 1000 $\mu\text{g/ml}$ for 24–72 h does not cause a significant increase in the proportion of dead cells. This indicates that the studied samples have a toxic, but not lethal effect on the cells.

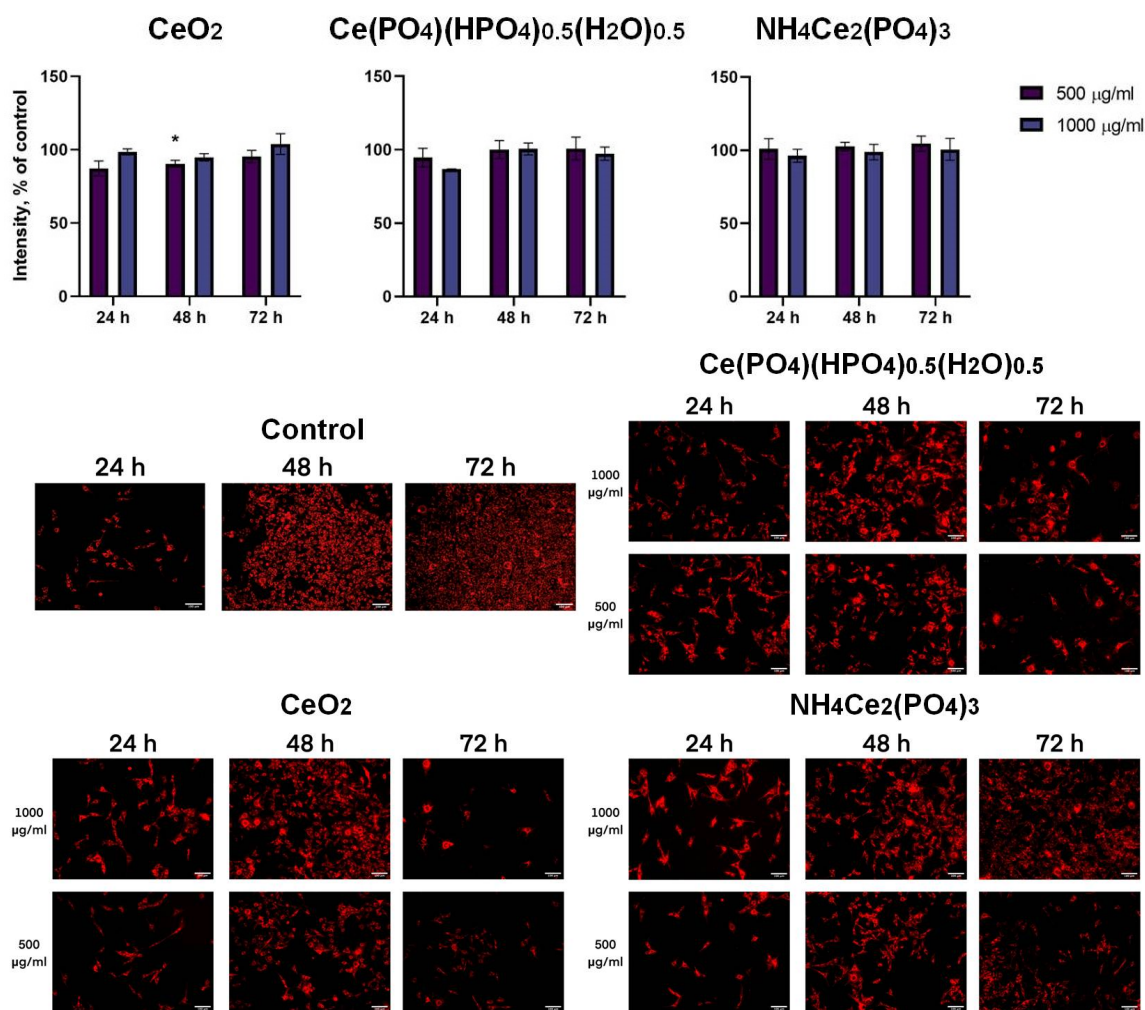


FIG. 5. Quantitative (top) and qualitative (bottom) analysis of the mitochondrial membrane potential level of B16/F10 murine melanoma cells *in vitro*. The assay was carried out after 24, 48 or 72 h of co-incubation of the cells with CeO₂ or cerium(IV) phosphates at concentrations of 500 and 1000 µg/ml. Scale bar – 100 µm

Cerium-containing nanobiomaterials are redox-active and can actively participate in redox reactions, exhibiting pro- or antioxidant properties depending on their microenvironment [43]. To establish the possible mechanism of the cytotoxic effect of cerium(IV) phosphates and nanocrystalline cerium dioxide on B16/F10 murine melanoma cells, we studied the mitochondrial membrane potential using the voltage-sensitive dye tetramethylrhodamine. The MMP level is inversely connected with the level of intracellular reactive oxygen species and oxidative stress state of the cells [44]. The data obtained indicate that the co-incubation of nanocrystalline ceria or cerium(IV) phosphates at concentrations of 500 and 1000 µg/ml with B16/F10 murine melanoma cells did not result in a significant decrease in the MMP level of the cells (Fig. 5a). At the same time, a qualitative assessment (Fig. 5b) shows that in the presence of CeO₂, Ce(PO₄)(HPO₄)_{0.5}(H₂O)_{0.5} or NH₄Ce₂(PO₄)₃ crystalline particles, the appearance of the cells changed. The increase in the size of the cells, changes in the number of outgrowths, and hypervascularization was observed. Such morphological changes are characteristic of apoptotic or senescent cells [45], being the markers of the toxicity.

Thus, within the framework of this work, the selective cytotoxicity of cerium(IV) phosphates to melanoma cells was assessed for the first time. It should be noted that, to date, selective cytotoxicity of nanocrystalline cerium dioxide to various types of cancer cells along with its protective action to normal cells was abundantly exemplified [46], but the mechanisms of such an effect are still under debate. Lysosomal injury [47], oxidative stress induction [48], interference with the nutrient transport functions of the membrane [49], and mechanical membrane disruption [50] are considered as the most probable reasons for the suppression of cancer cells viability by cerium dioxide. At the same time, there is no consensus on the factors initiating the cytotoxic effect, it can be associated with both the unique redox properties of nanosized CeO₂ [51] and redox-independent mechanisms involving the effect of free cerium ions in the cells microenvironment [52, 53]. In the latter case, the problem of solubility of ceric compounds in biological media is of high importance, but it is poorly discussed. In particular, Schwabe et al. [54] found that ceria nanoparticles release free cerium

species at pH below 4.6 and, in the presence of strong chelating agents, even at pH 8. Dahle et al. [55] showed that CeO₂ dissolution effect is significant at pH < 5 and is inversely proportional to surface area of the nanoparticles. Plakhova et al. [56] calculated the solubility product constant for ceria nanoparticles ($\log K_{sp} = -59.3 \pm 0.3$ in 0.01 M NaClO₄) and demonstrated that solubility behavior of CeO₂ in neutral and alkaline media is mostly pH independent, Ce(OH)_{4(aq)} being a predominant cerium form in aqueous solutions. Avramescu et al. [57] detected that solubility of CeO₂ nanoparticles at the 10 mg/l concentration in DMEM cell culture medium is significantly higher than in water.

Note that, for cerium(IV) phosphates, the data is even more scarce, the solubility of Ce(PO₄)(HPO₄)_{0.5}(H₂O)_{0.5} was reported to be lower than 1 mg/l in an aqueous medium at pH 1.3 [58], while in 1 M alkaline aqueous solution, the structure of this compound was reported to degrade completely due to the hydrolysis and the formation of Ce–O–Ce bonds [59].

Thus, it is obvious that in order to find the reasons for the selective cytotoxicity of different cerium(IV) phosphates, it is necessary to conduct comprehensive and detailed studies, including analysis of the chemical stability of cerium(IV) phosphates in biological media at various pH levels. However, the results obtained in this work can become a starting point for further studies of cerium(IV) phosphates, their possible inorganic UV filter applications, as well as their ability to counteract the negative delayed effects of ultraviolet irradiation associated with skin melanoma.

4. Conclusions

In this paper, we compared the cytotoxicity of nanoscale ceria and crystalline cerium(IV) phosphates Ce(PO₄)(HPO₄)_{0.5}(H₂O)_{0.5} or NH₄Ce₂(PO₄)₃ to B16/F10 murine melanoma cells *in vitro*. The toxicity was assessed at high concentrations of the solid particles, relevant to the content of inorganic components in sunscreen compositions. The MTT assay showed that the metabolic activity of B16/F10 murine melanoma cells decreases by about 40% after their contact with cerium(IV) phosphates, being even higher than for the CeO₂ nanoparticles. The IC₅₀ value was reached after 72 h of co-incubation of B16/F10 murine melanoma cells with ceria or ceric phosphates. The co-incubation of Ce(PO₄)(HPO₄)_{0.5}(H₂O)_{0.5}, NH₄Ce₂(PO₄)₃ or CeO₂ with cancer cells resulted in the changes in their morphology supporting the toxic effect of cerium-based materials to cancer cells. We believe that our results can also contribute to the understanding of the cytotoxicity of nanoscale CeO₂ in phosphate-rich biological media.

References

- [1] Achary S.N., Bevara S., Tyagi A.K. Recent progress on synthesis and structural aspects of rare-earth phosphates. *Coord. Chem. Rev.*, 2017, **340**, P. 266–297.
- [2] Behrsing T., Deacon G.B., Junk P.C. The chemistry of rare earth metals, compounds, and corrosion inhibitors. *Rare Earth-Based Corrosion Inhibitors*, Elsevier, Amsterdam, 2015, 1–37 p.
- [3] Sroor F.M.A., Edelmannand F.T. Tetravalent chemistry: Inorganic. *Rare Earth Elem. Fundam. Appl.*, John Wiley & Sons Ltd, Chichester, 2012, P. 313–320.
- [4] Scirè S., Palmisano L. *Cerium and cerium oxide: A brief introduction. Cerium Oxide (CeO₂): Synthesis, Properties and Applications*, Elsevier, Amsterdam, 2019, 1–12 p.
- [5] Montini T., Melchionna M., Monai M., Fornasiero P. Fundamentals and Catalytic Applications of CeO₂-Based Materials. *Chem. Rev.*, 2016, **116**(10), P. 5987–6041.
- [6] Mishra U.K., Chandel V.S., Singh O.P. A review on cerium oxide-based catalysts for the removal of contaminants. *Emergent Mater.*, 2022, **5**(5), P. 1443–1476.
- [7] Voncken J.H.L. *The Rare Earth Elements*. Springer International Publishing, Switzerland, 2016, 1–127 p.
- [8] Ermakov A., Popov A., Ermakova O., Ivanova O., Baranchikov A., Kamenskikh K., Shekunova T., Shcherbakov A., Popova N., Ivanov V. The first inorganic mitogens: Cerium oxide and cerium fluoride nanoparticles stimulate planarian regeneration via neoblastic activation. *Mater. Sci. Eng. C*, 2019, **104**, P. 109924.
- [9] Shcherbakov A.B., Reukov V.V., Yakimansky A.V., Krasnopeneva E.L., Ivanova O.S., Popov A.L., Ivanov V.K. CeO₂ Nanoparticle-Containing Polymers for Biomedical Applications: A Review. *Polymers*, 2021, **13**(6), P. 924.
- [10] Rajeshkumar S., Naik P. Synthesis and biomedical applications of Cerium oxide nanoparticles – A Review. *Biotechnol. Reports*, 2018, **17**, P. 1–5.
- [11] Egambaram O.P., Kesavan P.S., Ray S.S. Materials Science Challenges in Skin UV Protection: A Review. *Photochem. Photobiol.*, 2020, **96**(4), P. 779–797.
- [12] Parwaiz S., Khan M.M., Pradhan D. CeO₂-based nanocomposites: An advanced alternative to TiO₂ and ZnO in sunscreens. *Mater. Express*, 2019, **9**(3), P. 185–202.
- [13] Zholobak N.M., Shcherbakov A.B., Bogorad-Kobelska A.S., Ivanova O.S., Baranchikov A.Y., Spivak N.Y., Ivanov V.K. Panthenol-stabilized cerium dioxide nanoparticles for cosmeceutic formulations against ROS-induced and UV-induced damage. *J. Photochem. Photobiol. B*, 2014, **130**, P. 102–108.
- [14] Kolesnik I.V., Shcherbakov A.B., Kozlova T.O., Kozlov D.A., Ivanov V.K. Comparative Analysis of Sun Protection Characteristics of Nanocrystalline Cerium Dioxide. *Russ. J. Inorg. Chem.*, 2020, **65**(7), P. 960–966.
- [15] Gallagher R.P., Lee T.K. Adverse effects of ultraviolet radiation: A brief review. *Prog. Biophys. Mol. Biol.*, 2006, **92**(1), P. 119–131.
- [16] Gao Y., Chen K., Ma J.L., Gao F. Cerium oxide nanoparticles in cancer. *Onco. Targets. Ther.*, 2014, **7**, P. 835–840.
- [17] Shcherbakov A.B., Zholobak N.M., Spivak N.Y., Ivanov V.K. Advances and prospects of using nanocrystalline ceria in cancer theranostics. *Russ. J. Inorg. Chem.*, 2014, **59**(13), P. 1556–1575.
- [18] Mihai M.M., Holban A.M., Călugăreanu A., Orzan O.A. Recent advances in diagnosis and therapy of skin cancers through nanotechnological approaches. *Nanostructures Cancer Ther.*, 2017, P. 285–305.
- [19] Ali D., Alarifi S., Alkahtani S., AlKahtane A.A., Almalik A. Cerium Oxide Nanoparticles Induce Oxidative Stress and Genotoxicity in Human Skin Melanoma Cells. *Cell Biochem. Biophys.*, 2015, **71**(3), P. 1643–1651.

- [20] Aplak E., Von Montfort C., Haasler L., Stucki D., Steckel B., Reichert A.S., Stahl W., Brenneisen P. CNP mediated selective toxicity on melanoma cells is accompanied by mitochondrial dysfunction. *PLoS One*, 2020, **15**(1), P. e0227926.
- [21] Yong J.M., Fu L., Tang F., Yu P., Kuchel R.P., Whitelock J.M., Lord M.S. ROS-Mediated Anti-Angiogenic Activity of Cerium Oxide Nanoparticles in Melanoma Cells. *ACS Biomater. Sci. Eng.*, 2022, **8**(2), P. 512–525.
- [22] Ni P., Wei X., Guo J., Ye X., Yang S. On the origin of the oxidizing ability of ceria nanoparticles. *RSC Adv.*, 2015, **5**(118), P. 97512–97519.
- [23] De Marzi L., Monaco A., De Lapuente J., Ramos D., Borrás M., Di Gioacchino M., Santucci S., Poma A. Cytotoxicity and Genotoxicity of Ceria Nanoparticles on Different Cell Lines in Vitro. *Int. J. Mol. Sci.*, 2013, **14**(2), P. 3065–3077.
- [24] Singh S., Dosani T., Karakoti A.S., Kumar A., Seal S. Self W.T. A phosphate-dependent shift in redox state of cerium oxide nanoparticles and its effects on catalytic properties. *Biomaterials*, 2011, **32**(28), P. 6745–6753.
- [25] Rozhin P., Melchionna M., Fornasiero P., Marchesan S. Nanostructured Ceria: Biomolecular Templates and (Bio)applications. *Nanomaterials*, 2021, **11**(9), P. 2259.
- [26] Walther R., Huynh T.H., Monge P., Fruergaard A.S., Mamakhel A., Zelikin A.N. Ceria Nanozyme and Phosphate Prodrugs: Drug Synthesis through Enzyme Mimicry. *ACS Appl. Mater. Interfaces*, 2021, **13**(22), P. 25685–25693.
- [27] Yabe S., Sato T. Cerium oxide for sunscreen cosmetics. *J. Solid State Chem.*, 2003, **171**(1–2), P. 7–11.
- [28] Onoda H., Iwashita M. Synthesis of novel white pigments by shaking cerium compounds with phosphoric acid. *Emergent Mater.*, 2022.
- [29] Masui T., Hirai H., Imanaka N., Adachi G. New sunscreen materials based on amorphous cerium and titanium phosphate. *J. Alloys Compd.*, 2006, **408–412**, P. 1141–1144.
- [30] Wawrzynczak A., Feliczyk-Guzik A., Nowak I. Nanosunscreens: From nanoencapsulated to nanosized cosmetic active forms. *Nanobiomaterials Galen. Formul. Cosmet. Appl. Nanobiomaterials*, 2016, P. 25–46.
- [31] Seixas V.C., Serra O.A. Stability of sunscreens containing CePO₄: Proposal for a new inorganic UV filter. *Molecules*, 2014, **19**(7), P. 9907–9925.
- [32] De Lima J.F., Serra O.A. Cerium phosphate nanoparticles with low photocatalytic activity for UV light absorption application in photoprotection. *Dyes Pigm.*, 2013, **97**(2), P. 291–296.
- [33] Lima J.F., De Sousa Filho P.C., Serra O.A. Single crystalline rhabdophane-type CePO₄ nanoparticles as efficient UV filters. *Ceram. Int.*, 2016, **42**(6), P. 7422–7431.
- [34] Onoda H., Tanaka R. Synthesis of cerium phosphate white pigments from cerium carbonate for cosmetics. *J. Mater. Res. Technol.*, 2019, **8**(6), P. 5524–5528.
- [35] Sato T., Yin S. Morphology Control of Cerium Phosphates for UV-Shielding Application. *Phosphorus Res. Bull.*, 2010, **24**, P. 43–48.
- [36] Yin S., Saito M., Liu X., Sato T. Preparation and Characterization of Plate-like Cerium Phosphate / Nanosize Calcia Doped Ceria Composites by Precipitation Method. *Phosphorus Res. Bull.*, 2011, **25**, P. 68–71.
- [37] Sato T., Sato C., Yin S. Optimization of Hydrothermal Synthesis of Plate-Like Hydrated Cerium Phosphates and Their Photochemical Properties. *Phosphorus Res. Bull.*, 2008, **22**, P. 17–21.
- [38] Sato T., Li R., Sato C., Yin S. Synthesis and Photochemical Properties of Micaceous Cerium Phosphates. *Phosphorus Res. Bull.*, 2007, **21**, P. 44–47.
- [39] Kozlova T.O., Popov A.L., Kolesnik I.V., Kolmanovich D.D., Baranchikov A.E., Shcherbakov A.B., Ivanov V.K. Amorphous and crystalline cerium(IV) phosphates: biocompatible ROS-scavenging sunscreens. *J. Mater. Chem. B*, 2022, **10**(11), P. 1775–1785.
- [40] Baranchikov A.E., Polezhaeva O.S., Ivanov V.K., Tretyakov Y.D. Lattice expansion and oxygen non-stoichiometry of nanocrystalline ceria. *CrystrEngComm.*, 2010, **12**(11), P. 3531–3533.
- [41] Nazaraly M., Wallez G., Chanéac C., Tronc E., Ribot F., Quarton M., Jolivet J.P. The first structure of a cerium(IV) phosphate: Ab initio rietveld analysis of Ce^{IV}(PO₄)(HPO₄)_{0.5}(H₄O)_{0.5}. *Angew. Chemie - Int. Ed.*, 2005, **44**, P. 5691–5694.
- [42] Shekunova T.O., Istomin S.Y., Mironov A.V., Baranchikov A.E., Yapyntsev A.D., Galstyan A.A., Simonenko N.P., Gippius A.A., Zhurenko S.V., Shatalova T.B., Skogareva L.S., Ivanov V.K. Crystallization Pathways of Cerium(IV) Phosphates Under Hydrothermal Conditions: A Search for New Phases with a Tunnel Structure. *Eur. J. Inorg. Chem.*, 2019, **2019**(27), P. 3242–3248.
- [43] Yang Y., Mao Z., Huang W., Liu L., Li J., Li J., Wu Q. Redox enzyme-mimicking activities of CeO₂ nanostructures: Intrinsic influence of exposed facets. *Sci. Rep.*, 2016, **6**(1), P. 35344.
- [44] Suski J.M., Lebedzińska M., Bonora M., Pinton P., Duszynski J., Wieckowski M.R. Relation Between Mitochondrial Membrane Potential and ROS Formation. *Methods Mol. Biol.*, 2012, **810**, P. 183–205.
- [45] Kumari R., Jat P. Mechanisms of Cellular Senescence: Cell Cycle Arrest and Senescence Associated Secretory Phenotype. *Front. Cell Dev. Biol.*, 2021, **9**, P. 645593.
- [46] Shcherbakov A.B., Zholobak N.M., Ivanov V.K. Biological, biomedical and pharmaceutical applications of cerium oxide. *Cerium Oxide (CeO₂): Synthesis, Properties and Applications*, Elsevier, Amsterdam, 2020, P. 279–358.
- [47] Lin S., Wang X., Ji Z., Chang C.H., Dong Y., Meng H., Liao Y.-P., Wang M., Song T.-B., Kohan S., Xia T., Zink J.I., Lin S., Nel A.E. Aspect Ratio Plays a Role in the Hazard Potential of CeO₂ Nanoparticles in Mouse Lung and Zebrafish Gastrointestinal Tract. *ACS Nano*, 2014, **8**(5), P. 4450–4464.
- [48] Lin W., Huang Y., Zhou X.-D., Ma, Y. Toxicity of Cerium Oxide Nanoparticles in Human Lung Cancer Cells. *Int. J. Toxicol.*, 2006, **25**(6), P. 451–457.
- [49] Zeyons O., Thill A., Chauvat F., Menguy N., Cassier-Chauvat C., Oréar C., Daraspe J., Auffan M., Rose J., Spalla O. Direct and indirect CeO₂ nanoparticles toxicity for *Escherichia coli* and *Synechocystis*. *Nanotoxicology*, 2009, **3**(4), P. 284–295.
- [50] Rogers N.J., Franklin N.M., Apte S.C., Batley G.E., Angel B.M., Lead J.R., Baalousha M. Physico-chemical behaviour and algal toxicity of nanoparticulate CeO₂ in freshwater. *Environ. Chem.*, 2010, **7**(1), P. 50–60.
- [51] Pulido-Reyes G., Rodea-Palomares I., Das S., Sakthivel T.S., Leganes F., Rosal R., Seal S., Fernández-Pinás F. Untangling the biological effects of cerium oxide nanoparticles: The role of surface valence states. *Sci. Rep.*, 2015, **5**, P. 15613.
- [52] Caputo F., Giovanetti A., Corsi F., Maresca V., Briganti S., Licocchia S., Traversa E., Ghibelli L. Cerium oxide nanoparticles reestablish cell integrity checkpoints and apoptosis competence in irradiated HaCaT cells via novel redox-independent activity. *Front. Pharmacol.*, 2018, **9**, P. 1183.
- [53] Corsi F., Caputo F., Traversa E., Ghibelli L. Not only redox: The multifaceted activity of cerium oxide nanoparticles in cancer prevention and therapy. *Front. Oncol.*, 2018, **8**, P. 1–7.
- [54] Schwabe F., Schulin R., Rupper P., Rotzetter A., Stark W., Nowack B. Dissolution and transformation of cerium oxide nanoparticles in plant growth media. *J. Nanopart. Res.*, 2014, **16**, P. 2668.
- [55] Dahle J.T., Livi K., Arai Y. Effects of pH and phosphate on CeO₂ nanoparticle dissolution. *Chemosphere*, 2015, **119**, P. 1365–1371.
- [56] Plakhova T.V., Romanchuk A.Y., Yakunin S.N., Dumas T., Demir S., Wang S., Minasian S.G., Shuh D.K., Tyliczszak T., Shiryayev A.A., Egorov A.V., Ivanov V.K., Kalmykov S. N. Solubility of nanocrystalline cerium dioxide: Experimental data and thermodynamic modeling. *J. Phys. Chem. C*, 2016, **120**(39), P. 22615–22626.

- [57] Avramescu M.L., Chénier M., Beauchemin S., Rasmussen P. Dissolution Behaviour of Metal-Oxide Nanomaterials in Various Biological Media. *Nanomaterials*, 2023, **13**(1), P. 26.
- [58] Romanchuk A.Y., Shekunova T.O., Larina A.I., Ivanova O.S., Baranchikov A.E., Ivanov V.K., Kalmykov S.N. Sorption of Radionuclides onto Cerium(IV) Hydrogen Phosphate $\text{Ce}(\text{PO}_4)(\text{HPO}_4)_{0.5}(\text{H}_2\text{O})_{0.5}$. *Radiochemistry*, 2019, **61**(6), P. 719–723.
- [59] Kozlova T.O., Vasil'eva D.N., Kozlov D.A., Teplonogova M.A., Birichevskaya K.V., Baranchikov A.E., Gavrikov A.V., Ivanov V.K. On the Chemical Stability of $\text{Ce}^{\text{IV}}(\text{PO}_4)(\text{HPO}_4)_{0.5}(\text{H}_2\text{O})_{0.5}$ in Alkaline Media. *Russ. J. Inorg. Chem.*, 2022, **67**(12), P. 1901–1907.

Submitted 6 February 2023; accepted 31 March 2023

Information about the authors:

Taisiya O. Kozlova – Kurnakov Institute of General and Inorganic Chemistry of the Russian Academy of Sciences, Moscow, Russia; ORCID 0000-0002-9757-9148; taisia.shekunova@yandex.ru

Anton L. Popov – Institute of Theoretical and Experimental Biophysics of the Russian Academy of Sciences, Pushchino, Russia; ORCID 0000-0003-2643-4846; antonpopovleonid@gmail.com

Mikhail V. Romanov – Institute of Theoretical and Experimental Biophysics of the Russian Academy of Sciences, Pushchino, Russia; rmvya@yandex.ru

Irina V. Savintseva – Institute of Theoretical and Experimental Biophysics of the Russian Academy of Sciences, Pushchino, Russia; savintseva.irina@mail.ru

Darya N. Vasilyeva – Kurnakov Institute of General and Inorganic Chemistry of the Russian Academy of Sciences, Moscow, Russia; National Research University Higher School of Economics, Moscow, Russia; dnavasileva_1@edu.hse.ru

Alexander E. Baranchikov – Kurnakov Institute of General and Inorganic Chemistry of the Russian Academy of Sciences, Moscow, Russia; ORCID 0000-0002-2378-7446; a.baranchikov@yandex.ru

Vladimir K. Ivanov – Kurnakov Institute of General and Inorganic Chemistry of the Russian Academy of Sciences, Moscow, Russia; ORCID 0000-0003-2343-2140; van@igic.ras.ru

Conflict of interest: the authors declare no conflict of interest.